

See discussions, stats, and author profiles for this publication at: <https://www.researchgate.net/publication/231180121>

Thermal Evolution of Carbon-Supported Pd Nanoparticles Studied by Time-Resolved X-ray Diffraction

ARTICLE · AUGUST 2001

DOI: 10.1021/jp011093p

CITATIONS

18

READS

15

5 AUTHORS, INCLUDING:



Patrizia Canton

Università Ca' Foscari Venezia

96 PUBLICATIONS 1,597 CITATIONS

SEE PROFILE



C. Meneghini

Università Degli Studi Roma Tre

170 PUBLICATIONS 1,834 CITATIONS

SEE PROFILE



Pietro Riello

Università Ca' Foscari Venezia

115 PUBLICATIONS 1,408 CITATIONS

SEE PROFILE



Antonella Balerna

INFN - Istituto Nazionale di Fisica Nucleare

84 PUBLICATIONS 1,041 CITATIONS

SEE PROFILE

Thermal Evolution of Carbon-Supported Pd Nanoparticles Studied by Time-Resolved X-ray Diffraction

Patrizia Canton,^{*,†} Carlo Meneghini,[‡] Pietro Riello,[†] Antonella Balerna,[§] and Alvis Benedetti[†]

Dipartimento di Chimica Fisica, Università degli studi Cà Foscari, Via Torino 158, I-30170 Venezia-Mestre, and Calle Larga S. Marta 2137, I-30123 Venezia, Università degli studi di "Roma Tre", Via della Vasca Navale 84, I-00147 Roma, INFN-Laboratori Nazionali di Frascati, Via E. Fermi 40, I-00044 Frascati (RM), Italy, and Istituto Nazionale di Fisica della materia, CRG-GILDA c/o ESRF, BP 220, F-38043 Grenoble, France

Received: March 22, 2001; In Final Form: June 18, 2001

Time-resolved X-ray diffraction measurements were performed in situ on a Pd/C catalyst during two successive thermal treatments from 300 to 873 K. Analysis of the diffraction patterns, as a function of thermal treatment, reveals anomalous features in the evolution of Pd particles. An intermediate $\text{Pd}_{1-x}\text{C}_x$ phase ($x \sim 0.1$) is observed and dissolved into pure Pd at ~ 700 K. Moreover, the size of metal particles, remaining almost constant (~ 10 nm) during the annealing, abruptly increases to 30 nm in close connection with the dissolution of the $\text{Pd}_{1-x}\text{C}_x$ phase. These effects clearly point out an interaction between the metal and the support and suggest that the formation of the $\text{Pd}_{1-x}\text{C}_x$ phase would prevent the metal-particle sintering, thus maintaining the catalyst dispersion at a high level. There is no evidence of the formation of a $\text{Pd}_{1-x}\text{C}_x$ phase during the second temperature treatment since only metallic Pd was detected. As for the growth in particle size, a small increase to 32 nm was observed.

1. Introduction

Palladium is an important catalyst that is used both in industrial processes and in laboratory practice. Usually, it is dispersed as small particles (nanometer size) on inert matrixes by chemical procedures: a larger surface-to-volume ratio improves the reactivity and efficiency and reduces the amount of active metal employed. The determination of particle sizes and structural modifications when depending on the preparation methods, thermal treatments, and during a chemical reaction, are fundamental issues in characterizing this class of materials. The characterization of these materials is often difficult since the high metal dilution represents a serious limitation for several experimental techniques. Chemisorption-based techniques imply the hypothesis of the absorption stoichiometry. Transmission electron microscopy (TEM) analysis requires the counting of a huge number of particles to be representative of the sample; this is a time-consuming task that has evident intrinsic limitations in following a kinetic evolution. X-ray diffraction (XRD) methods, like XRD line-broadening analysis and small-angle X-ray scattering (SAXS), can give detailed information on atomic structure and particle size. Unfortunately, the intense, diffuse background that is scattered from the support partially masks the signal relative to the supported catalyst phases, making it difficult to extract the structural information.

Recently, some of us^{1,2} studied carbon-supported Pd particles (Pd/C) using the anomalous small-angle X-ray scattering (ASAXS) technique and a modified approach of the Rietveld structural refinement of X-ray powder diffraction patterns. These measurements showed that XRD could give a very detailed

picture of both the structure and the microstructure of highly dispersed metallic phases. A-SAXS and conventional XRD experiments require long counting times, so it is not possible to probe in situ the effects of thermal treatments on the structure of the metallic phase. Nevertheless, this information could be important for the comprehension of the chemical behavior of these catalysts.

The intense and brilliant X-ray sources available on the synchrotron radiation facilities, coupled with area detectors such as imaging plate (IP), allow high-quality time-resolved X-ray diffraction (TR-XRD) experiments.³ In this way, it is possible to follow the evolution of the metal particles as a function of temperature and/or chemical reaction.

These experiments could explain the mechanisms of aging processes observed during catalyst performance that result in a progressive reduction of the catalyst efficiency. These processes could have several causes such as metal-particle sintering (reducing the surface-to-volume ratio of the active phase) and/or catalyst poisoning; moreover, an interaction with the support could play a relevant role.

The aim of this work is to investigate in situ the structural and microstructural evolution of Pd phases on a Pd/C catalyst as a function of thermal treatment, in a wide temperature range, using the TR-XRD technique. In fact, although several studies have been published on these catalysts, little is known about the structural evolution of the catalyst under annealing and the effects produced by the interaction between the metal and the support.

2. Experimental Methods

2.1. Sample Preparation. A commercial active carbon, derived from coconut shell, with a surface area of 1200 m²/g and a pore volume of 0.60 mL/g, was used as the support. The catalyst was obtained by the impregnation of carbon with an aqueous solution of Na_2PdCl_4 and the reduction by $\text{H}_2\text{NaO}_2\text{P}$.

* To whom correspondence should be addressed. E-mail: cantonpa@unive.it.

[†] Università degli studi Cà Foscari. E-mail: riello@unive.it, benedetti@unive.it.

[‡] Istituto Nazionale di Fisica della materia and Università degli studi di "Roma Tre". E-mail: meneghini@fis.uniroma3.it.

[§] INFN-Laboratori Nazionali di Frascati. E-mail: balerna@lnf.infn.it.

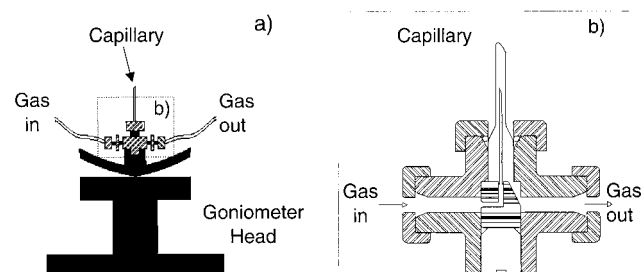


Figure 1. (a) Sketch showing the T-Swagelok piece mounted on the goniometer head. (b) Enlargement of the boxed area in panel a showing details of the modified T-Swagelok piece: the gas enters the Swagelok and flows through a Teflon cylinder and through a needle that is inserted into the capillary sample holder.

H₂O at 298 K. The metal weight fraction (Pd 0.66 wt %) was determined by atomic mass spectroscopy (Perkin-Elmer model 500).

2.2. Time-Resolved X-ray Powder Diffraction. TR-XRD patterns were collected at the Italian GILDA⁴ (General Italian Line for Diffraction and Absorption) beamline at the European Synchrotron Radiation Facility (ESRF) using a translating IP⁵ and a reaction chamber to control the gas flow through the sample (Figure 1). The high linearity and low (electronic) background make IP detectors very attractive for investigating highly diluted supported materials. The translating IP setup available on the GILDA beamline employs a 200 (*h*) × 400 (*v*) mm² IP. The IP support linearly translates behind two vertical slits selecting a narrow (*w* = 4 mm) portion of the Debye rings, and a continuous series of diffractograms are collected as a function of time and sample treatment. The data stored in the latent image are recovered and digitized using a Fuji BAS-2500 laser scanner with a 100 × 100 μm² pixel size and a dynamic range of 16 bit/pixel. Pd/C samples are contained in a pure amorphous quartz capillary (*d*_{cap} = 1 mm) mounted on a modified Swagelok T-piece. A needle (Figure 1b) fluxes the gas through the sample during the thermal treatment. The T-piece was mounted on a goniometer head (Huber), allowing an accurate alignment on the beam. The capillary oscillates (±180°) around its axis during the data acquisition to improve the grain orientation statistics. Sample heating was achieved using a gas flow heater (Cyberstar, Grenoble, France) whose temperature was previously calibrated by measuring, in the same experimental conditions, the thermal lattice expansion of an annealed Ag powder sample (325 mesh, Aldrich).

X-ray beam size was 2 (*h*) × 1.5 (*v*) mm², and the sample-to-IP distance (*D*_o) was 303 mm. The instrumental line broadening ($\Delta_{2\theta}$) is mainly determined by the capillary diameter and the sample-to-IP distance:³

$$\Delta_{2\theta} \approx \frac{180}{\pi} \frac{d_{\text{cap}}}{D_o} \cos(2\theta) \quad (1)$$

We verified the validity of this formula by collecting, in the same experimental conditions, diffraction patterns of a reference sample (c-Si, NIST).

Preliminary XRD characterization, performed on a conventional diffractometer (Cu K α radiation), showed that the metal was partially oxidized. For this reason, the catalyst was reduced under H₂ flux for 1 h at room temperature (RT) and washed with N₂ for 3 h, and finally, TR-XRD measurements were performed under continuous N₂ flux.

In-situ TR-XRD patterns (λ = 0.62016) were collected during successive thermal treatments of the Pd/C catalyst with tem-

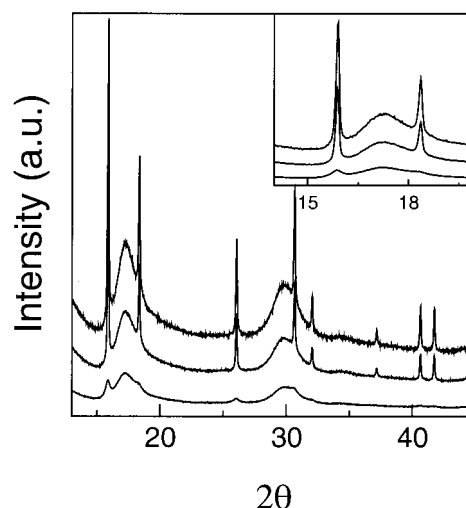


Figure 2. Data collected in the full-plate mode taken at room temperature. From the bottom: raw data of the as prepared catalyst and of the sample after the first and second temperature ramps (TT1, TT2). In the inset, the enlargement shows the 111 and 200 Pd Bragg reflections.

perature ramps between 300 and 873 K. The first treatment (TT1) was performed with a heating rate of 2.3 K/min, the second (TT2) with a heating rate of 4.8 K/min. Between TT1 and TT2 the sample was cooled to RT. Diffractograms were collected at RT before and after each temperature scan using the full IP. In such a way, we obtained high-quality (low-noise) diffraction patterns to be used as references for the initial and final sample structures (Figure 2).

To improve data analysis (see Results), we measured an empty capillary and a capillary containing only the carbon support using the same procedure (two ramps TT1 and TT2) used for Pd/C measurements. In such a way, we were able to check for possible modifications of the support, induced by thermal treatment, that could affect the analysis of the data. These measurements point out that, within the experimental uncertainty, the thermal treatments do not affect the structure of the carbon support.

The digitized images collected in the full-plate mode were integrated using the FIT2D program⁶ to have intensity vs 2θ diffraction patterns. TR-XRD patterns were extracted by integrating the rectangular stripes⁷ of the digitized images (Figure 3).

Integrated XRD patterns (both full-plate and time-resolved measurements) were analyzed using the Rietveld structural refinement method as implemented in the DBWS9006 program.⁸

3. Results

Figure 2 reports the XRD patterns collected at RT in the full-plate mode. The raw data indicate a single Pd metallic phase (with no evidence of Pd oxidation) having an fcc structure (Fm $\bar{3}$ m spatial group, Pd in the 0,0,0 special position) with *a* = 0.3889 nm. Temperature treatments do not affect the metallic phase but clearly induce Pd particle growth, as is evident from the sharpening of the diffraction peaks (Figure 2).

Powder diffraction patterns, relative to those at selected temperatures of the first thermal treatment (TT1), are reported in Figure 4, highlighting the region of the most intense Pd Bragg peaks.

Even from a qualitative examination, an unusual trend of the Pd phase contribution is evident: at lower temperatures (*T* < 500 K), Pd Bragg peaks shift to small angles, showing a Pd

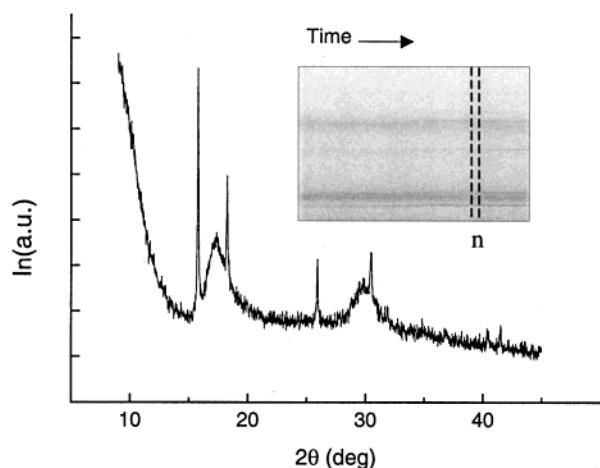


Figure 3. Digitized image of the first temperature ramp: the dotted lines represent the n th integration stripe. The XRD pattern obtained by the integration is shown.

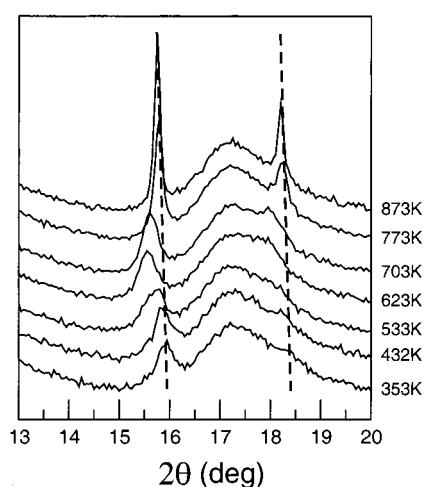


Figure 4. Powder diffraction patterns, relative to those at selected temperatures of the first (TT1) thermal treatment, highlighting the region of the most intense Pd Bragg peaks (111 and 200 reflections). The dotted lines show the peak shift as expected from thermal dilation only.

lattice expansion as expected from a thermal dilation effect. Above ~ 550 K, there is a sudden, larger expansion of the Pd lattice that cannot be ascribed to a purely thermal expansion effect. Moreover, increasing T above 670 K, we observed that the Pd lattice rapidly contracts.

Figure 5 reports an example of Rietveld structural refinement for the pattern collected at 477 K: Bragg peaks relative to the fcc Pd phase are evident but superimposed on an intense, diffuse background coming from the carbon support and the sample holder. Figure 6 reports the lattice parameter, $a_i(T)$ ($i = \text{TT1, TT2}$), relative to the metallic phase, together with the theoretical⁹ Pd lattice parameter $a_{\text{Pd}}(T)$ as a function of temperature. As already observed, in the temperature range between 550 and 700 K, the lattice parameter of the metallic phase clearly departs from the expected values for pure Pd. At $T > 700$ K, there is a contraction of $a_{\text{TT1}}(T)$ that recovers the expected values of the pure metal. The results obtained for the second temperature scan show that $a_{\text{TT2}}(T)$ closely follows $a_{\text{Pd}}(T)$ in the whole temperature range.

Figure 6 also reports the volume-weighted mean size, $D_{\text{TT1}}(T)$, of metal crystallites. The crystallite dimensions were calculated by line-broadening analysis using a procedure that combines best-fitting and Fourier analysis.^{10,11} This method

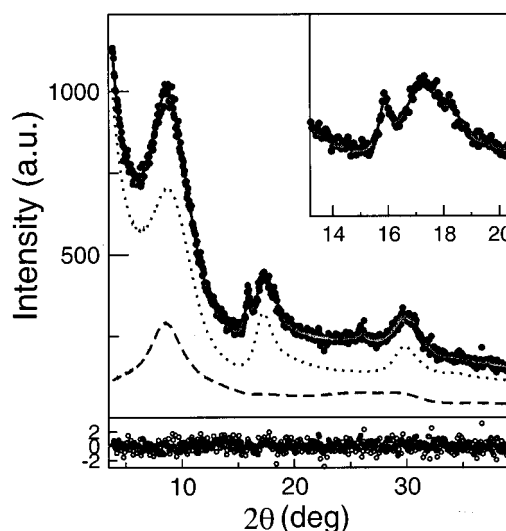


Figure 5. Rietveld refinement for the pattern collected at 477 K: the circle represents the experimental data, the continuous line the fitted data. The dotted and segmented lines represent the contributions of the carbon support and capillary, respectively. These two contributions were used in the refinement to describe the background scattering. In the inset, an enlargement of the abscissa shows the 111 and 200 Pd Bragg peaks, together with the hump ($\sim 17.5^\circ$) due to the carbon support. At the bottom, the weighted residuals are reported (open circles).

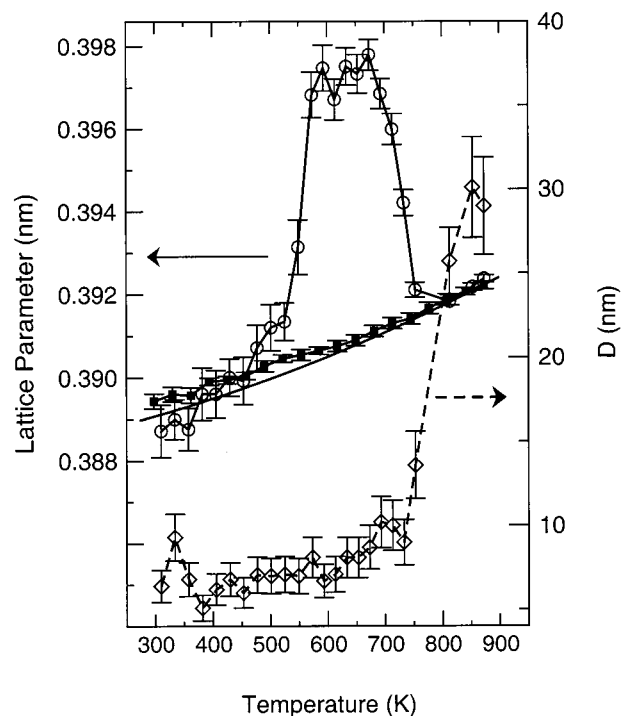


Figure 6. Evolution of the Pd lattice parameters during the first (open circles) and the second (closed squares) temperature ramp. The continuous line represents the theoretical Pd lattice expansion. The crystallite dimensions (open diamonds) obtained during the first temperature scan are also shown.

deconvolutes the instrumental line broadening from the experimental profile and attributes the remaining broadening only to size effects.

4. Discussion

TR-XRD data collected during TT1 point out an anomalous expansion of the lattice parameter of the metallic phase in the

range between 550 and 700 K. The thermal treatment only affects the cell volume and grain size (Figure 6), while there is no evidence of phases other than the fcc phase. To interpret this effect, we supposed that, upon heat treatments >500 K, something goes into the Pd lattice and is then eliminated when the temperature is raised to >700 K. The inclusion of both H (β -PdH phase) and C ($\text{Pd}_{1-x}\text{C}_x$ solid solutions¹²) into the Pd lattice enlarges the cell volume, keeping the fcc structure. The diffraction pattern collected before TT1 clearly demonstrates that the starting sample, after being washed in N_2 , did not contain any residual β -PdH. The anomalous trend observed for $a_{\text{TT1}}(T)$ must indicate the inclusion of C into the Pd lattice, producing a $\text{Pd}_{1-x}\text{C}_x$ solid solution. Palladium carbide, in fact, has a fcc structure,¹² and its formation has been documented^{12,13} in flows of CO, ethylene, or acetylene on heated Pd. The same authors also reported that PdC is metastable and decomposes at $T > 873$ K. The occurrence of several types of carbon-rich compounds on the surface of active carbons has been proven by many independent methods of analysis.¹⁵ These carbonilic groups come from the precursor material, from which the active carbon has been produced. This is especially true for carbons obtained from raw materials rich in oxygen due to their incomplete carbonization. Tarkovskaya et al.¹⁶ proposed a model of the active carbon surface in which the surface is rich in COO- and CH- functional groups. The interaction of Pd particles with these functional groups should be responsible for the formation of $\text{Pd}_{1-x}\text{C}_x$ solution.

Neutron diffraction studies and EXAFS measurements^{12,17} indicate that C occupies the octahedral sites of the fcc lattice, thus enlarging the cell volume. The amount of C included in the structure depends on the preparation procedure, and the cell edge grows linearly with carbon concentration ($a = a_0 + 6.9E - 02 \times x$, where a_0 is the pure Pd lattice parameter).¹²⁻¹⁴ In our case, the amount of carbon absorbed into the Pd lattice cannot be directly determined since XRD is not very sensitive to light elements, especially in the presence of heavy scatterers such as Pd. Nevertheless, assuming the linear thermal dilation of Pd and PdC to be similar, we can estimate, from the lattice parameter, the amount of C present in the $\text{Pd}_{1-x}\text{C}_x$ structure that results ($0.09 \leq x \leq 0.10$). The maximum amount of carbon atoms in $\text{Pd}_{1-x}\text{C}_x$, as reported in the literature, is $x = 0.15$, obtained by fluxing the sample with a gas rich in carbon compounds such as CO.

The values obtained in our case indicate an unsaturated $\text{Pd}_{1-x}\text{C}_x$ solution; nevertheless, the values are quite large, which suggests that a relevant amount of residual carbonilic groups exists in the "as prepared" catalyst.

With regard to particle size, the as prepared sample shows Pd particles of ca. 6 nm. Upon heating the metal, we observed that the particle size remains almost constant until ca. 730 K; then, it grows rapidly as a function of temperature, attaining an average size of ca. 30 nm for $T \geq 850$ K. The evolution of $a_{\text{TT1}}(T)$ and $D_{\text{TT1}}(T)$ shows that the collapse of the lattice parameter (expulsion of C from PdC) and the growth of Pd particles are strictly related phenomena. This suggests that the inclusion of carbon into the Pd lattice inhibits the crystallite growth process, keeping the catalyst particle dispersion constant; as soon as C is expelled, the pure Pd particles are free to grow and/or coalesce.

The lattice parameter a_{TT2} and particle size D_{TT2} do not present anomalies: a_{TT2} closely follows the lattice expansion curve calculated from the pure-Pd linear-expansion coefficient. $D_{\text{TT2}}(T)$ slightly increases from 30 to 32 nm.

There could be different reasons for this behavior: on one hand, the former thermal treatment under N_2 flux removed most of the carbonilic groups present on the support; on the other hand, the growth of Pd particles (that occurred during the first TT1 scan) reduced the interaction between Pd and C.

5. Conclusion

We have investigated the structural evolution of Pd phases in Pd/C catalysts as a function of annealing temperature. Our results showed the formation of an intermediate PdC solution in the temperature range of 500–700 K that dissolves into pure Pd upon raising the annealing temperature.

The growth of Pd particles seems to be one of the mechanisms responsible for the aging effect exhibited by these compounds. On the contrary, it is difficult to evaluate the influence of Pd–C interaction on the chemical reactivity of the catalyst only on the basis of XRD data. In fact, if the inclusion of C preserves the surface/volume ratio, keeping a high particle dispersion, the formation of a PdC phase could affect the chemical reactivity of the catalyst.

Acknowledgment. Financial support from Murst (60%) is acknowledged. The GILDA project is financed by Italian institutions INFN, INFN, and CNR. The technical support from F. Campolungo, F. Danca, V. Sciarra, and V. Tullio is greatly appreciated. Prof. F. Pinna and Dr. N. Pernicone are gratefully acknowledged for their helpful discussions.

References and Notes

- (1) Benedetti, A.; Polizzi, S.; Riello, P.; Pinna, F.; Goerigk, G. *J. Catal.* **1997**, *171*, 345.
- (2) Riello, P.; Canton, P.; Benedetti, A. *Langmuir* **1998**, *14*, 6617.
- (3) Norby, P. *J. Appl. Crystallogr.* **1997**, *30*, 21.
- (4) Pascarelli, S.; Boscherini, F.; D'Acapito, F.; Hrđy, J.; Meneghini, C.; Mobilio, S. *J. Synchrotron Radiat.* **1996**, *3*, 147.
- (5) Meneghini, C.; Artioli, G.; Balerna, A.; Gualtieri, A. F.; Norby, P.; Mobilio, S. *J. Synchrotron Radiat.* Submitted for publication.
- (6) Hammersley, A. P.; Svensson, S. O.; Thomson, A. *Nucl. Instrum. Methods Phys. Res., Sect. A* **1994**, *346*, 321.
- (7) A modified version of the original ScanT8 program written by G. Artioli and P. Norby (unpublished) was used.
- (8) Sakthivel, A.; Young, R. *User's Guide to Programs DBWS-9600PC*; School of Physics, Georgia Institute of Technology: Atlanta, GA, 1990.
- (9) Grigoriev; Mejlhøf *Physical Constants* Moskva, **1991**.
- (10) Enzo, S.; Polizzi, S.; Benedetti, A. *Z. Kristallogr.* **1995**, *170*, 275.
- (11) Benedetti, A.; Fagherazzi, G.; Enzo, S.; Battagliarin, M. *J. Appl. Crystallogr.* **1988**, *21*, 543.
- (12) Ziemecki, S. B.; Jones, G. A.; Swartzfager, D. G.; Harlow, R. L. *J. Am. Chem. Soc.* **1985**, *107*, 4547.
- (13) Maciejewski, M.; Baiker, A. *J. Phys. Chem.* **1994**, *98*, 285.
- (14) Siller, R. H.; McLellan, R. B.; Rudee, M. L. *J. Less-Common Met.* **1969**, *18*, 432.
- (15) Jankowska, H.; Swiatkowski, A.; Choma, J. *Active Carbon*; Hellis Horwood Limited: Chichester, England, and Wydawnictwa Naukowo-Techniczne: Warsaw, Poland, 1991; Chapter 3.
- (16) Tarkovskaya, I. A.; Strazhesko, D. N.; Goba, W. E. *Adsorbts. i Adsorbenty* **1977**, *5*, 3.
- (17) McCaulley, J. A. *Phys. Rev. B* **1993**, *47*, 4873.